

Structure and crystallization behaviour of amorphous $\text{Bi}_{0.96}\text{Pb}_{0.24}\text{SrCaCu}_{1.6}\text{O}_{5+x}$ high-temperature superconductor material

Y. KHAN

Institut für Werkstoffe der Elektrotechnik, Ruhr-Universität Bochum, 4630 Bochum 1, Germany

Pb-doped Bi-Sr-Ca-Cu-O superconductor materials are of great technological importance because of their high superconducting transition temperatures (T_c) [1]. Although most of the Pb escapes during sintering of these Pb-doped materials [2, 3], additions of Pb are necessary to produce high- T_c Bi-Sr-Ca-Cu-O superconducting compounds. The solid-state reaction method is usually used for the preparation of superconducting materials on the basis of this quinary system [1-3]. However, in recent years the method of crystallization from the amorphous materials (obtained by rapidly quenching the melts) with subsequent heat-treatment of the crystallized product has led to homogeneous good-quality Bi-Sr-Ca-Cu-O superconducting materials ([4, 5] and references cited therein). In order to understand the crystallization kinetics, the crystallization behaviour of these amorphous materials was investigated by a continuous heating-cooling process, as is the case for the dynamic temperature X-ray diffraction (DTXD) [6] and differential thermal analysis (DTA) methods. Results are reported for the $\text{Bi}_{0.96}\text{Pb}_{0.24}\text{SrCaCu}_{1.6}\text{O}_{5+x}$ compound ($0 < x < 1$).

About 20 g of a mixture of $\text{Bi}_{0.96}\text{Pb}_{0.24}\text{SrCaCu}_{1.6}\text{O}_{5+x}$, containing appropriate amounts of the starting materials Bi_2O_3 , PbO_2 , SrCO_3 , CaCO_3 and CuO , was thoroughly mixed in a planetary agate mortar using ethanol as lubricant. The dried mixture was fired at 1025 ± 5 K in air for 2 h in alumina crucibles in a muffle furnace. The product was ground in a hand agate mortar and heated at 1075 ± 5 K for 16 h in the same way as above. The last treatment was repeated two or three times in order to ensure homogeneity. The final product was ground and melted in Pt crucibles in air in a muffle furnace at 1350-1375 K. The viscous melt was quenched in air by squeezing it between two rapidly rotating Cu rollers (each about 5 cm in diameter and 10 cm in length) in contact with each other. In this way thin flakes (about 10-30 mm long, 5-15 mm wide and 40-100 μm thick) were obtained, which were found to be X-ray amorphous. Microanalysis and X-ray fluorescence analysis showed that more than half of the total weighed amount of Pb was lost during the whole preparation process.

For room-temperature X-ray diffraction analysis, an Enraf-Nonius Guinier camera was used. High-temperature X-ray diffraction analysis was carried out in a dynamic vacuum of 10^{-1} - 10^{-4} Pa at a heating rate of 50 K h^{-1} by DTXD [6], using $\text{Cu K}\alpha$

radiation. It should be mentioned that due to continuity of the diffraction lines along the ordinate in a DTXD pattern, even minute details become visible. X-ray diffraction intensities were measured by a modified microcomputer-controlled Zeiss-Jena MD100 microdensitometer. Thermal anomalies corresponding to structural changes detected in the DTXD pattern were recorded by a modified DTA instrument using Pt crucibles and under conditions similar to those in the DTXD method.

The rapidly quenched $\text{Bi}_{0.96}\text{Pb}_{0.24}\text{SrCaCu}_{1.6}\text{O}_{5+x}$ ($0 < x < 1$) material was found to be amorphous by X-ray diffraction methods, characterized by the presence of three diffraction haloes in its X-ray diffraction pattern, however with intensity sequence weak, strong and weak (Figs 1 and 2) in contrast with the Fraunhofer diffraction haloes (having intensity sequence very strong, very weak and very very weak) expected for the conventional Bernal-type amorphous solids [7, 8]. Similar X-ray diffraction results have been reported for amorphous Mg-Zn alloys [9]. The weighted averages of these three diffraction haloes could be indexed by means of conventional crystallography on the basis of a perovskite-type cubic unit cell with lattice parameter $a = 0.426(3)$ nm (Fig. 2 and Table I), implying that this amorphous material was not of the Bernal-type, but must have consisted of microcrystals 10-15 unit cells (of the perovskite-type) in size as calculated from the breadth of the diffraction haloes using the Scherrer formula [10]. The X-ray diffraction pattern reported by Chaudhuri *et al.* [5] for the amorphous Bi-Sr-Ca-Cu-oxides has also been found to contain three diffraction haloes with the same intensity sequence as found for the amorphous $\text{Bi}_{0.96}\text{Pb}_{0.24}\text{SrCaCu}_{1.6}\text{O}_{5+x}$ compound in this work.

The weak, sharp X-ray diffraction lines (marked with q in Fig. 1) were due to some unreacted CaO in the sample. These X-ray diffraction lines were always detected for these amorphous materials at high cooling rates without, however, having any influence on the shape or size of the intensity sequence of the diffraction haloes due to the amorphous state of these materials.

Dynamic temperature crystallization, i.e. crystallization upon continuously varying temperature as is the case during continuously heating-cooling in DTXD or DTA, revealed that this amorphous material crystallizes at 685 ± 2 K (Figs 1 and 3). The crystal structure of the first product of crystallization was highly distorted, as is seen from the broadness of

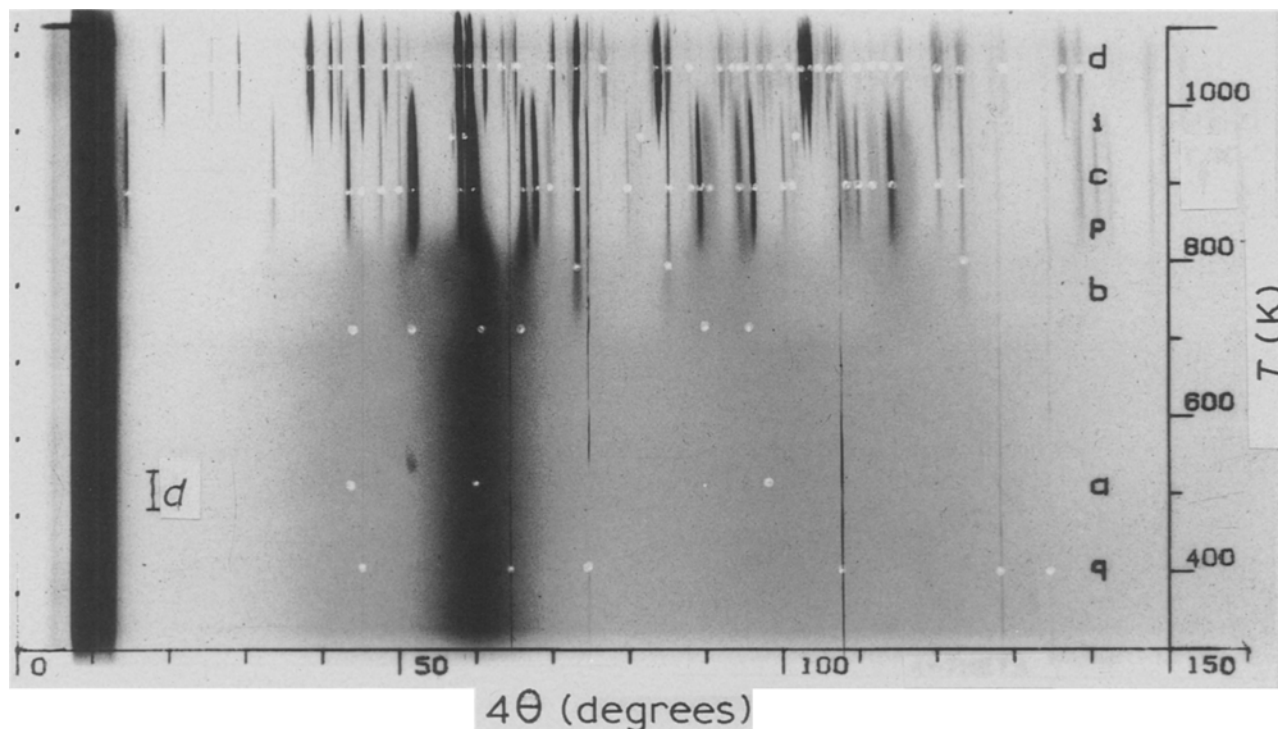


Figure 1 DTXD pattern of the amorphous $\text{Bi}_{0.96}\text{Pb}_{0.24}\text{SrCaCu}_{1.6}\text{O}_{5+x}$ flakes ($\text{Cu K}\alpha$ radiation, 30 kV and 40 mA) taken at a heating rate of 50 K h^{-1} in a dynamic vacuum of 10^{-4} Pa. X-ray diffraction lines marked with white dots on a horizontal line belong to the phase designated by lower case letters on the right (explained in the text). Black dots along the ordinate on the left are the primary beam marks 100°C apart. The slit width is given by d on the left.

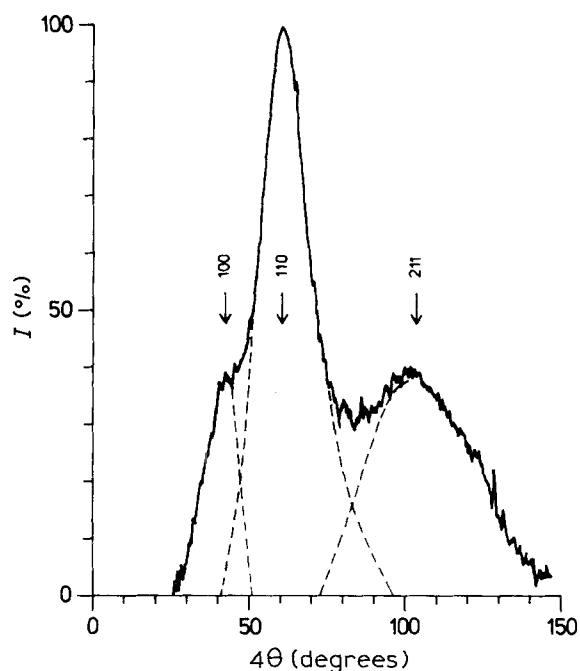


Figure 2 Microdensitometer scan at 400 K of the DTXD pattern shown in Fig. 1. The Miller indices (hkl) are based on a perovskite-type cubic unit cell.

TABLE I Structure data (at room temperature) of the amorphous phase marked a in Fig. 1. System, cubic of the perovskite-type; lattice parameter, $a = 0.426(4)$ nm; remark, since the corresponding X-ray diffraction lines were extraordinarily broad (Fig. 2), weighted averages of these lines are given here

hkl	$\sin^2 \theta_0$	$\sin^2 \theta_c$	I_0 (%)
100	0.0332	0.0326	20
110	0.0659	0.0652	100
211	0.1956	0.1956	30

the corresponding X-ray diffraction lines (marked b in Fig. 1) and was found to be of the 2.4 nm Bi-based superconducting compound type (Table II). At slightly higher temperature (i.e. at 693–695 K) a perovskite-type compound having lattice parameter $a = 0.427(7)$ nm formed (p in Fig. 1, Table III). At about 825 K the material recrystallized and the regular 2.4 nm Bi-based superconducting compound formed (c in Fig. 1), which decomposed at about 1020 K. However, shortly before the 2.4 nm Bi-based phase decomposed a new unstable phase (marked i in Fig. 1) was found to form at about 925 K. Finally, a new tetragonal phase with lattice parameters $a = 0.7255(9)$ nm and $c = 7.363(5)$ nm (marked d in Fig. 1, Table IV) formed at about 978 K. The corresponding thermal reaction was found to be endothermic by DTA and existed over a wide temperature range of 978–1020 K (Fig. 3). This reaction could be attributed to loss of oxygen because DTA and DTXD were carried out in dynamic vacuum (i.e. evacuating the sample chamber continuously) at a low heating rate (50 K h^{-1}).

Although this material has been found to melt at about 1063 K (as is seen from the DTA curve in Fig. 3 and diffuseness of some corresponding X-ray diffraction lines in Fig. 1), the X-ray diffraction lines remained extremely sharp up to 1115 K, i.e. about 50 K above the melting temperature (Fig. 1), implying that a well-defined long-range crystalline order corresponding to the phase (marked d in Fig. 1) must exist in the melt of this material. The melt solidified at about 1043 K upon cooling, giving rise to a broad exothermic peak (Fig. 3).

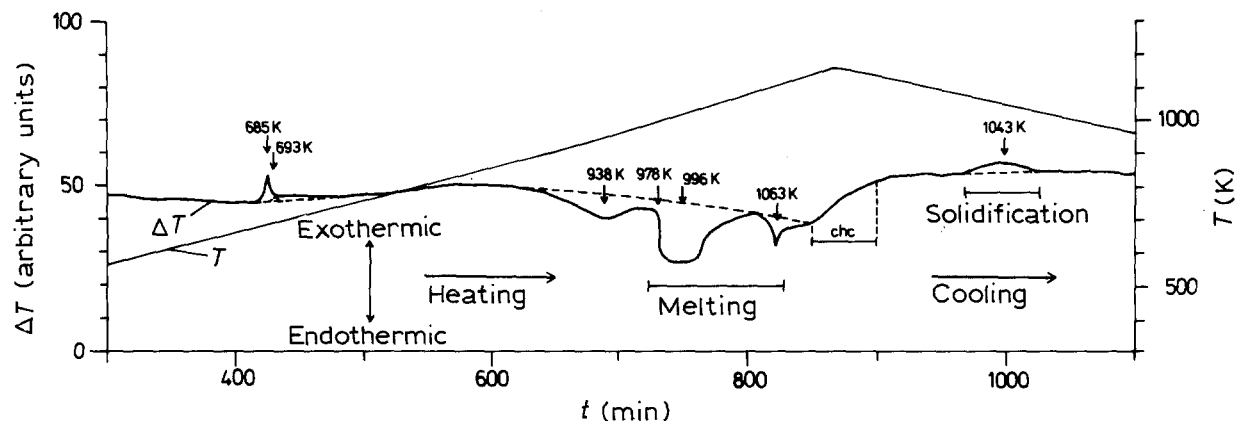


Figure 3 DTA analysis of the amorphous $\text{Bi}_{0.96}\text{Pb}_{0.24}\text{SrCaCu}_{1.6}\text{O}_{5+x}$ compound. chc, Change-over from heating to cooling.

TABLE II Structure data (at about 730 K) of the phase marked b in Fig. 1. System, tetragonal; lattice parameters, $a = 0.4967(8)$ nm, $c = 2.456(6)$ nm, $c/a = 4.492(6)$

hkl	$\sin^2 \theta_0$	$\sin^2 \theta_c$	I_0 (%)
006	0.0364	0.0355	10
104		0.0356	
113	0.0478	0.0486	10
107	0.0681	0.0681	100
200	0.0795	0.0795	20
0010	0.0981	0.0985	30
0012	0.1418	0.1418	10
1111	0.1590	0.1589	10
200		0.1590	

TABLE III Structure data (at about 750 K) of the phase marked p in Fig. 1. System, cubic of the perovskite-type; lattice parameter, $a = 0.4271$ (7) nm; remark, note that only fcc-type reflexes have so far been detected

hkl	$\sin^2 \theta_0$	$\sin^2 \theta_c$	I_0 (%)
111	0.0986	0.0986	100
200	0.1314	0.1315	50
220	0.2630	0.2630	20
311	0.3618	0.3616	10

TABLE IV Structure data (at about 1075 K) of the phase marked d in Fig. 1. System, tetragonal; lattice parameters, $a = 0.7255(9)$ nm, $c = 7.363(5)$ nm, $c/a = 10.14(8)$

hkl	$\sin^2 \theta_0$	$\sin^2 \theta_c$	I_0 (%)
008	0.0069	0.0070	50
013	0.0123	0.0123	30
0012	0.0159	0.0158	40
117	0.0278	0.0279	80
0016		0.0281	
119	0.0317	0.0315	50
1110	0.0338	0.0335	40
1112	0.0381	0.0384	75
0117	0.0432	0.0430	40
0020		0.0438	
1018	0.0465	0.0468	10
204		0.0469	
206	0.0487	0.0491	5
217	0.0621	0.0618	100
119		0.0621	
1022	0.0648	0.0643	80
219		0.0653	
0123	0.0692	0.0693	50
2111		0.0697	

TABLE IV Cont.

0026		0.0741	
1024	0.0745	0.0744	30
2113		0.0750	
1122	0.0761	0.0756	5
1214	0.0782	0.0779	30
220	0.0903	0.0903	50
2119	0.0955	0.0960	5
2027	0.0981	0.0982	60
0030		0.0986	
2210	0.1013	0.1013	50
033	0.1028	0.1026	5
037	0.1071	0.1070	20
0315	0.1267	0.1262	60
0034		0.1267	
1226	0.1306	0.1305	50
0133		0.1306	
326	0.1514	0.1507	20
237		0.1521	
239	0.1558	0.1556	5
2131	0.1622	0.1618	10
3212		0.1625	
3214	0.1680	0.1682	<5
1232	0.1690	0.1687	5
2034	0.1720	0.1719	<5
400	0.1806	0.1806	<5
2319	0.1860	0.1863	60
2230	0.1894	0.1889	60
144	0.1939	0.1936	<5
0329		0.1938	
417	0.1977	0.1973	20
1140		0.1979	
2232	0.2026	0.2025	20
1410		0.2028	
1044	0.2244	0.2235	5
4020		0.2244	
4119	0.2314	0.2315	20
2238	0.2489	0.2486	30
4125	0.2605	0.2604	20
3040	0.2769	0.2770	5
2046		0.2771	
502	0.2828	0.2826	5
3327		0.2831	
519	0.3026	0.3024	<5
2244		0.3025	
5113	0.3127	0.3120	50
2339		0.3134	
0519	0.3216	0.3218	30
3240		0.3221	
4139	0.3588	0.3586	5
2517		0.3590	

From the above discussion it follows that the dynamic temperature crystallization behaviour of amorphous $\text{Bi}_{0.96}\text{Pb}_{0.24}\text{SrCaCu}_{1.6}\text{O}_{5+x}$ is quite complex. A number of metastable or unstable phases form up to the melting temperature. There is strong evidence for the existence of a long-range crystalline order in the liquid state of this type of materials. No Bernal-type structure was found for amorphous $\text{Bi}_{0.96}\text{Pb}_{0.24}\text{SrCaCu}_{1.6}\text{O}_{5+x}$ solid.

References

1. T. ISHIDA, T. SAKUMA, T. SASAKI and Y. KAWADA, *Jpn. J. Appl. Phys.* **28** (1989) L559.
2. M. TAKANO, J. TAKADA, K. ODA, H. KITAGUCHI, Y. MUIRA, Y. IKEDA, Y. TOMII and H. MAZAKI,

ibid. **27** (1988) L1041.

3. S. BHAN, Y. KHAN and S. ROTHAEEMEL, *Supercond. Sci. Technol.* **2** (1989) 265.
4. T. KOMATSU, R. SATO, C. HIROSE, K. MATSUDA and T. YAMASHITA, *Jpn. J. Appl. Phys.* **27** (1988) L2293.
5. B. K. CHAUDHURI, K. SAM and S. P. S. GUPTA, *J. Mater. Sci. Lett.* **8** (1989) 520.
6. Y. KHAN, *J. Phys. E: Scient. Instrum.* **18** (1985) 1054.
7. J. D. BERNAL, *Proc. R. Soc.* **A280** (1964) 299.
8. G. S. CARGILL III, in "Diffraction studies in non-crystalline substances", edited by I. Hargittai and W. J. Orville (Elsevier, Amsterdam, 1981) p. 753.
9. Y. KHAN, *J. Mater. Sci.* **24** (1989) 963.
10. A. GUINIER, "X-ray diffraction" (Freeman, London, 1963).

*Received 11 March
and accepted 14 September 1992*